

See discussions, stats, and author profiles for this publication at: <https://www.researchgate.net/publication/231452401>

Bis(nitroxyl) radical adducts of rhodium(II) and molybdenum(II) carboxylate dimers: Magnetic exchange interactions propagated by metal-metal bonds

ARTICLE *in* JOURNAL OF THE AMERICAN CHEMICAL SOCIETY · SEPTEMBER 1984

Impact Factor: 12.11 · DOI: 10.1021/ja00330a069

CITATIONS

20

READS

23

4 AUTHORS, INCLUDING:



David Hendrickson

University of California, San Diego

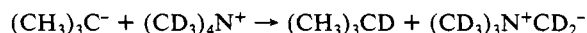
599 PUBLICATIONS 26,782 CITATIONS

SEE PROFILE

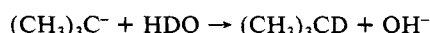
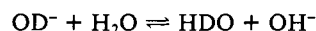
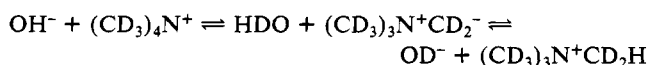
bromide at a mercury pool cathode, under the same conditions as those used to record polarograms, yield isobutane (43%), isobutylene (44%), and 2,2,3,3-tetramethylbutane (9%) as major products at a potential (-1.40 V) corresponding to the first polarographic wave, whereas isobutane (50%) and isobutylene (47%) are the predominant species obtained from electrolyses at a potential (-1.70 V) on the plateau of the second polarographic wave. Product distributions at each potential do not vary for concentrations of water between 5 and 50 mM. In addition, the apparent coulometric n value is essentially unity regardless of potential, although evidence to be published elsewhere¹ demonstrates that the *tert*-butyl carbanion is indeed the intermediate produced at a potential (-1.70 V) corresponding to the second polarographic wave; the apparent n value of 1 at the more negative potential is due to the fact that approximately one-half of the alkyl bromide undergoes a non-electron-consuming, base-promoted dehydrohalogenation.

When an electrolysis of 2.5 mM *tert*-butyl bromide was performed at -1.70 V in unlabeled solvent-supporting electrolyte containing 5 mM H₂O and 50 mM D₂O, 42% of the isobutane was determined (by means of mass spectrometry) to be monodeuterated. If we assume a kinetic isotope ratio (k_H/k_D) of 1.25, a figure based on the work of de la Torre and Sease,² we estimate that approximately 47% of the *tert*-butyl carbanions generated by electrolysis of the starting material at -1.70 V are protonated by water (at a concentration of 55 mM in the solvent-supporting electrolyte). We know from previous investigations that higher concentrations of water (present as D₂O) protonate even larger percentages of electrogenerated alkyl carbanions; in dimethylformamide containing 0.1 M tetramethylammonium perchlorate and 1 M D₂O, 82% of the decane derived from 1-iododecane³ and 66% of the octane obtained from 2-iodooctane⁴ are deuterated. Our results with *tert*-butyl bromide show clearly that electrogenerated *tert*-butyl carbanions must be protonated by species in the system other than water.

Perdeuterated tetramethylammonium perchlorate ((CD₃)₄NClO₄) was prepared from (CD₃)₄NCl by metathesis with silver perchlorate. An electrolysis of 2.5 mM *tert*-butyl bromide at -1.70 V in dimethylformamide containing 0.1 M (CD₃)₄NClO₄ and approximately 15 mM H₂O gave the expected yield of isobutane, 34% of which was found to be monodeuterated. One can question whether deuterons from (CD₃)₄N⁺ enter the H₂O pool via a sequence of protonation-deprotonation (scrambling) reactions, thereby becoming available as HDO or D₂O to form monodeuterated isobutane from electrogenerated *tert*-butyl carbanions. We have tested this possibility in a separate chemical experiment with a solution initially containing 30 mM (CD₃)₄NClO₄, 15 mM OH⁻ in the form of (CH₃)₄NOH·5H₂O, and 15 mM H₂O in dimethylformamide. By the time (CH₃)₄NOH·5H₂O dissolved—approximately 60 min (comparable to the duration of an exhaustive electrolysis of *tert*-butyl bromide)—NMR spectra recorded with the aid of a Nicolet NT-360 instrument revealed that the extent of deuterium scrambling was only 24% of the theoretical maximum. When all the preceding results are considered together, we conclude that the transfer of protons (deuterons) from tetramethylammonium cations to *tert*-butyl carbanions takes place *directly*



as well as *indirectly* via proton (deuteron) scrambling:



(5) La Perriere, D. M.; Carroll, W. F., Jr.; Willett, B. C.; Torp, E. C.; Peters, D. G. *J. Am. Chem. Soc.* **1979**, *101*, 7561-7568.

(6) Mbarak, M. S.; Peters, D. G. *J. Org. Chem.* **1982**, *47*, 3397-3403.

As a consequence of proton (deuteron) scrambling, the experimentally measured yields of monodeuterated isobutane formed in the presence of various sources of deuterons do not indicate the relative rates of *direct* proton (deuteron) donation to the *tert*-butyl carbanion by these species.

Another electrolysis was done at -1.70 V with a 2.5 mM solution of (CD₃)₃CBr in unlabeled dimethylformamide containing 0.1 M (CH₃)₄NClO₄ and 8 mM H₂O; 5% of the resulting isobutane⁷ was found to be (CD₃)₃CD, which could originate via attack of (CD₃)₃C⁻ on unreduced (CD₃)₃CBr. Perdeuterated dimethylformamide (DCON(CD₃)₂) was used as solvent for the electrolysis of 2.5 mM *tert*-butyl bromide at -1.70 V in the presence of 0.1 M (CH₃)₄NClO₄ and 14 mM H₂O; no more than 1% of the resulting isobutane was monodeuterated.

We are intrigued by the likelihood that an ylide (trimethylammonium methylide) is formed by deprotonation of the supporting-electrolyte cation and by the prospect that electrolyses of alkyl halides (at potentials corresponding to the production of carbanion intermediates) in dimethylformamide containing tetramethylammonium perchlorate could afford a way to generate the ylide for other chemical purposes.

(7) It is also possible that a small quantity of (CD₃)₃CD originates from disproportionation of (CD₃)₃C[•] radicals, which are generated because of imperfect control of the electrolysis potential at -1.70 V.

Bis(nitroxyl) Radical Adducts of Rhodium(II) and Molybdenum(II) Carboxylate Dimers: Magnetic Exchange Interactions Propagated by Metal-Metal Bonds

Teng-Yuan Dong and David N. Hendrickson*

School of Chemical Sciences, University of Illinois
Urbana, Illinois 61801

Timothy R. Felthouse* and Huey-Sheng Shieh

Corporate Research Laboratories, Monsanto Company
St. Louis, Missouri 63167

Received March 26, 1984

Interactions between paramagnetic centers connected by a continuous bonding framework provide models for thermal and photochemical processes¹ and probes into the transition metal to ligand orbital interface.² The magnitude of such a magnetic exchange interaction, gauged by the exchange parameter J , contains sensitive information about the electronic structure of the atomic or molecular bridging moiety connecting the two paramagnets. The effectiveness of an extended bridging group to propagate an exchange interaction offers insight into possible pathways of electron transfer in solution redox reactions (whether of the inner- or outer-sphere type),³ in biological electron-transport chains,⁴ and in mixed-valence compounds.⁵ The existence of a

(1) Goldberg, A. H.; Dougherty, D. A. *J. Am. Chem. Soc.* **1983**, *105*, 284-290 and references therein.

(2) For recent reviews, see: (a) Hendrickson, D. N. In "Magneto-Structural Correlations in Exchanged Coupled Systems"; Willett, R. D.; Gatteschi, D.; Kahn, O., Eds.; Reidel: Boston, 1984. (b) Milaeva, E. R.; Rubezhov, A. Z.; Prokofev, A. I.; Okhlobystin, O. Yu. *Usp. Khim.* **1982**, *51*, 1638-1673; *Russ. Chem. Rev. (Engl. Transl.)* **1982**, *51*, 942-960. (c) Laronov, S. V. *Zh. Strukt. Khim.* **1982**, *23*, 125-147; *J. Struct. Chem.* **1982**, *23*, 594-617. (d) Eaton, S. S.; Eaton, G. R. *Coord. Chem. Rev.* **1978**, *26*, 207-262.

(3) (a) Haim, A. *Pure Appl. Chem.* **1982**, *55*, 89-98; *Prog. Inorg. Chem.* **1983**, *30*, 273-357. (b) Francesconi, L. C.; Corbin, D. R.; Clauss, A. W.; Hendrickson, D. N.; Stucky, G. D. *Inorg. Chem.* **1981**, *20*, 2059-2069.

(4) McGourty, J. L.; Blough, N. V.; Hoffman, B. M. *J. Am. Chem. Soc.* **1983**, *105*, 4470-4472 and references therein.

(5) "Mixed-Valence Compounds, Theory and Applications in Chemistry, Physics, Geology, and Biology"; Brown, D. B., Ed.; Reidel: Boston, 1980.

distance-dependence limit to superexchange interactions^{2a,3b,6} constitutes a topic of continuing theoretical interest. In this paper we present a novel modification to the classical dimeric metal carboxylate structure⁷ in which nitroxyl radicals are coordinated through the axial positions of the diamagnetic dirhodium(II)⁸ and dimolybdenum(II)⁹ tetracarboxylates. The results afford the first examples of magnetic exchange interactions *through* metal-metal bonds. The magnitudes of these interactions were completely unexpected in terms of the radical pair separations (vide infra).

Four new coordinated nitroxyl biradicals have been prepared having the general formula $M_2(O_2CR)_4(\text{Tempo})_2$, in which the carboxylate ligands are the perfluorinated derivatives of acetate (1, $M = \text{Rh}$, $R = \text{CF}_3$; 4, $M = \text{Mo}$, $R = \text{CF}_3$), butyrate (2, $M = \text{Rh}$, $R = \text{C}_3\text{F}_7$), or benzoate (3, $M = \text{Rh}$, $R = \text{C}_6\text{F}_5$) and the axial nitroxyl ligands are 2,2,6,6-tetramethylpiperidiny-1-oxy (Tempo). The molecular structures of two of the dirhodium(II) biradical complexes (1 and 2) have been determined by single-crystal X-ray diffraction techniques.¹⁰ The structure of $\text{Rh}_2(\text{O}_2\text{CCF}_3)_4(\text{Tempo})_2$ (1) illustrated in Figure 1 consists of a typical⁸ centrosymmetric rhodium carboxylate dimer coordinated at each axial site by a nitroxyl oxygen atom with a Rh-O distance of 2.220 (2) Å. The Rh-Rh bond length of 2.417 (1) Å is in accord with previous structures of this type.⁸ The closest *intra*-molecular separation (O...O) of the radical ligands in 1 is 6.853 (3) Å. A structure similar to 1 in composition was recently reported¹² for $\text{Cu}_2(\text{O}_2\text{CCl}_3)_4(\text{Tempo})_2$, but this shows severe distortions of the typical $M_2(\text{O}_2\text{CR})_4L_2$ framework. The structure of the analogous perfluorobutyrate complex $\text{Rh}_2(\text{O}_2\text{CC}_3\text{F}_7)_4(\text{Tempo})_2$ (2) has also been determined¹⁰ and displays the same dimeric architecture as 1 with a Rh-Rh bond of 2.424 (1) Å and axial bonds to the Tempo oxygen atoms of 2.238 (5) Å in length. The critical difference in the structures of 1 and 2 occurs in the shortest *inter*molecular contacts (O...N) between neighboring Tempo ligands that increase from 4.706 (3) Å in 1 to 6.219 (8) Å in 2, in line with the molecular packing requirements of the bulkier heptafluorobutyrate ligands. Finally, a critical comparison of the X-ray powder diffraction patterns for 1 and $\text{Mo}_2(\text{O}_2\text{CCF}_3)_4(\text{Tempo})_2$ (4) suggests that these compounds are isomorphous.

Variable-temperature (4.2–350 K) magnetic susceptibility data were collected for compounds 1–4 and $\text{Rh}_2(\text{O}_2\text{CCF}_3)_4(\text{Tempo})_2$ (5),¹³ where Tempo represents 4-hydroxy-2,2,6,6-tetramethylpiperidiny-1-oxy. For each of the rhodium-Tempo biradicals, an astonishingly large antiferromagnetic exchange interaction is observed. For 1 the effective magnetic moment per nitroxyl group decreases gradually from 1.06 μ_B at 342 K, to 0.80 μ_B at 250 K, and finally to 0.14 μ_B at 80 K at which point the compound is essentially diamagnetic. A good least-squares fit of the magnetic susceptibility data can be obtained using the expression for an $S_1 = S_2 = 1/2$ dimer.¹⁴ The antiferromagnetic coupling is

characterized by $J = -239 \text{ cm}^{-1}$ in an $\hat{H} = -2\hat{S}_1\hat{S}_2$ Hamiltonian. Evidence for the intramolecularity of this interaction in 1 comes from the magnitude of the exchange interaction found in 2 ($J = -269 \text{ cm}^{-1}$), which is larger than that found for 1 in spite of the considerably greater intermolecular nitroxyl-nitroxyl contact distance. Compound 3 also displays strong antiferromagnetic coupling between coordinated radical centers, but the interaction ($J = -184 \text{ cm}^{-1}$) is somewhat weaker than found for 1 and 2. However, just as the exchange interactions in the above three rhodium biradicals were unexpectedly large,¹⁵ the $\text{Mo}_2(\text{O}_2\text{CCF}_3)_4(\text{Tempo})_2$ magnetic susceptibility data surprisingly display no signs of an interaction down to 4.2 K, which indicates that $|J| \lesssim 0.5 \text{ cm}^{-1}$. Finally, magnetic susceptibility data for the crystallographically characterized¹³ compound 5 indicate that the compound behaves as a simple paramagnet with no exchange interaction detectable to 4.2 K. In 5 the hydroxyl substituents of the Tempo ligands coordinate to both axial sites of $\text{Rh}_2(\text{O}_2\text{CCF}_3)_4$ while the nitroxyl groups from adjacent dimers participate in hydrogen bonding to the hydroxyl hydrogen atoms. In this structure both the intra- and intermolecular interactions are weak.

The magnitude of the *intra*molecular antiferromagnetic exchange interaction in 1–3 is not only unusual in light of the more than 6.8-Å distance between radical centers but it also exceeds the $J = -142 \text{ cm}^{-1}$ interaction reported¹⁶ for the copper acetate monohydrate dimer, $\text{Cu}_2(\text{O}_2\text{CCH}_3)_4(\text{H}_2\text{O})_2$. The Cu...Cu separation in this complex is 2.61 (1) Å,¹⁷ and the exchange interaction is believed¹⁸ to arise from a superexchange interaction propagated by the acetate bridging ligands.

The remarkable ability of the Rh-Rh single bond to propagate a sizeable exchange interaction between the coordinated nitroxyl groups compared to the inability of *any* interaction to develop across the Mo-Mo quadrupole bond can be understood from a qualitative consideration of the metal-metal bonding energy levels obtained from SCF-X α -SW calculations on $\text{Rh}_2(\text{O}_2\text{CH})_4(\text{H}_2\text{O})_2$ ¹⁹ and $\text{Mo}_2(\text{O}_2\text{CH})_4$,²⁰ and how these levels interface with nitroxyl group orbitals.²¹ The effect of the electron-withdrawing CF_3 substituents should lead to a relatively constant downshifting of energy levels in both $M_2(\text{O}_2\text{CR})_4L_2$ molecules. This has the practical consequence^{22,23} of improving adduct formation by decreasing the energy separation between the metal orbitals and the axial ligand atom lone pair orbitals. For rhodium the electronic

(14) The magnetic susceptibility data for compounds 1–3 were corrected for temperature-independent paramagnetism (TIP) and diamagnetism at each temperature by subtracting the susceptibility of the corresponding diamagnetic rhodium carboxylate complex. The corrected molar paramagnetic susceptibilities (χ_M) of 1–3 were then least-squares fit to the following equation:

$$\chi_M = \frac{Ng^2\beta^2}{kT} \left[\frac{2}{3 + \exp(-2J/(kT))} \right]$$

In the case of one complex, 3, there was evidence of a small amount of a paramagnetic impurity, as indicated by a magnetic susceptibility that increased somewhat below ~80 K.

(15) From a solution study of the monoadduct between $\text{Rh}_2(\text{O}_2\text{CCF}_3)_4$ and Tempo, the extent of delocalization of the unpaired electron onto the dirhodium centers appears small in so far as distinct coupling to only one of the two rhodium atoms was reported. As seen from the exchange interactions for 1–3, a completely different picture emerges for the solid-state biradical complexes examined here. See: Richman, R. M.; Kuechler, T. C.; Tanner, S. P.; Drago, R. S. *J. Am. Chem. Soc.* **1977**, *99*, 1055–1058.

(16) Doedens, R. J. *Prog. Inorg. Chem.* **1976**, *21*, 209–230.

(17) (a) DeMeester, P.; Fletcher, S. R.; Skapski, A. C. *J. Chem. Soc., Dalton Trans.* **1973**, 2575–2578. (b) Brown, G. M.; Chidambaram, R. *Acta Crystallogr., Sect. B* **1973**, *B29*, 2393–2403.

(18) DeLoth, P.; Cassoux, P.; Daudey, J. P.; Malvien, J. P. *J. Am. Chem. Soc.* **1981**, *103*, 4007–4016.

(19) (a) Norman, J. G., Jr.; Kolari, H. J. *J. Am. Chem. Soc.* **1978**, *100*, 791–799. (b) Christoph, G. G.; Koh, Y.-B. *J. Am. Chem. Soc.* **1979**, *101*, 1422–1434.

(20) Norman, J. G., Jr.; Kolari, H. J.; Gray, H. B.; Trogler, W. C. *Inorg. Chem.* **1977**, *16*, 987–993.

(21) Beck, W.; Schmidtner, K.; Keller, H. J. *Chem. Ber.* **1967**, *100*, 503–511.

(22) Drago, R. S.; Long, J. R.; Cosmano, R. *Inorg. Chem.* **1982**, *21*, 2196–2202.

(23) Cotton, F. A.; Norman, J. G., Jr. *J. Am. Chem. Soc.* **1972**, *94*, 5697.

(6) Coffman, R. E.; Buettner, G. R. *J. Phys. Chem.* **1979**, *83*, 2387–2392.

(7) (a) Bleaney, B.; Bowers, K. D. *Proc. R. Soc. London, Ser. A* **1952**, *214*, 451–465. (b) Van Niekerk, J. N.; Schoening, F. K. L. *Nature (London)* **1953**, *171*, 36–37; *Acta Crystallogr.* **1953**, *6*, 227–232.

(8) Recent reviews of Rh_2^{4+} complexes include: (a) Felthouse, T. R. *Prog. Inorg. Chem.* **1982**, *29*, 73–166. (b) Cotton, F. A.; Walton, R. A. "Multiple Bonds Between Metal Atoms"; Wiley: New York, 1982; Chapters 7, 8. (c) Boyar, E. B.; Robinson, S. D. *Coord. Bonds Rev.* **1983**, *50*, 109–208.

(9) For a comprehensive review of Mo_2^{4+} complexes, see ref 8b, Chapters 3 and 8.

(10) Tables of atomic positional parameters are available as supplementary material; complete details will be published elsewhere.¹¹ Crystallographic data are as follows: 1, $\text{Rh}_2(\text{O}_2\text{CCF}_3)_4(\text{Tempo})_2$, space group $P\bar{1}$; $a = 8.715$ (2) Å, $b = 10.765$ (3) Å, $c = 11.501$ (3) Å; $\alpha = 107.18$ (2)°, $\beta = 103.30$ (2)°, $\gamma = 107.61$ (2)°; $d_{\text{calc}} = 1.751 \text{ g cm}^{-3}$; $Z = 1$; final residuals $R_1 = 0.035$, $R_2 = 0.044$ for 2479 reflections with $I > 2.33\sigma(I)$. 2, $\text{Rh}_2(\text{O}_2\text{CC}_3\text{F}_7)_4(\text{Tempo})_2$, space group $P2_1/c$; $a = 11.478$ (3) Å, $b = 16.911$ (4) Å, $c = 13.280$ (5) Å; $\beta = 90.61$ (2)°; $d_{\text{calc}} = 1.766 \text{ g cm}^{-3}$; $Z = 2$; current residuals $R_1 = 0.112$, $R_2 = 0.159$ for 3201 reflections with $I > 2.33\sigma(I)$.

(11) Dong, T.-Y.; Hendrickson, D. N.; Felthouse, T. R.; Shieh, H.-S., manuscript in preparation.

(12) Porter, L. C.; Dickman, M. H.; Doedens, R. J. *Inorg. Chem.* **1983**, *22*, 1962–1964.

(13) Cotton, F. A.; Felthouse, T. R. *Inorg. Chem.* **1982**, *21*, 2667–2675.

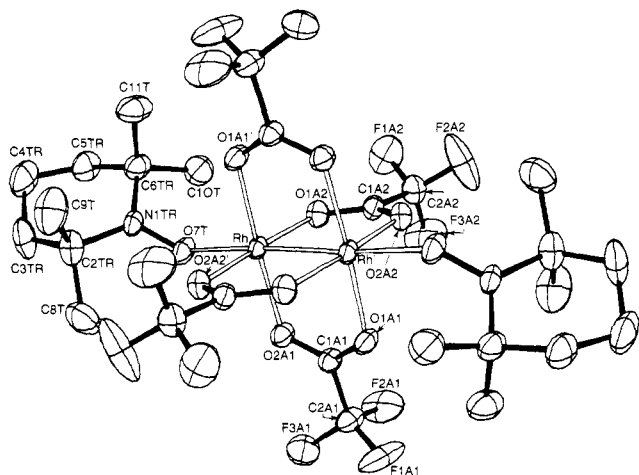


Figure 1. Molecular structure of $\text{Rh}_2(\text{O}_2\text{CCF}_3)_4(\text{Tempo})_2$ (**1**) with thermal ellipsoids shown at the 50% probability level. Primed atoms are related to unprimed ones by a center of inversion located at the midpoint of the Rh-Rh bond.

ground-state configuration is extraordinarily sensitive to the identity of the adduct atoms,²⁴ but for oxygen donors like H_2O or Tempo the configuration is $\pi^4\sigma^2\delta^2\pi^*\delta^2$.¹⁹ The long axial Rh-O bond distances (2.22–2.29 Å) found here and in other $\text{Rh}_2(\text{O}_2\text{CCF}_3)_4\text{L}_2$ structures⁸ reflect a weak σ donor interaction that is not expected to contribute significantly to the superexchange pathways for the Tempo radicals in **1**–**3**. However, the greater electronegativity of Rh compared to Mo¹⁹ combined with the filled antibonding orbitals for Rh in $\text{M}_2(\text{O}_2\text{CR})_4\text{L}_2$ compounds affords an effective π -back-bonding interaction with axial donors, and it is the energetic proximity and correct orbital symmetry that allows the filled Rh-Rh π^* orbitals to interact with the Tempo nitroxyl π^* orbitals containing the unpaired electrons. From the structures of **1** and **2** above, the C_2NO planes make dihedral angles of 47–52° with the equatorial carboxylate oxygen O_4 planes at distances of 2.22–3.29 Å. Complete spin pairing is known to occur in solid-state nitroxyl dimers²⁵ separated by up to 3.2 Å, an interaction that occurs through overlap of the $\pi^*-\pi^*$ orbitals.

For $\text{Mo}_2(\text{O}_2\text{CCF}_3)_4(\text{Tempo})_2$ the nitroxyl oxygen lone pair is expected to interact very weakly with the Mo atoms in line with the insensitivity of the Mo_2^{4+} unit to axial donors.^{8,26} More importantly, all of the low-lying orbitals are filled in the $\sigma^2\pi^4\delta^2$ ground-state configuration involved in Mo-Mo and Mo-O-(carboxylate) bonding. No orbitals drop into the proper range^{19,20} to interact with the nitroxyl π^* orbitals containing the unpaired electrons, and as such the quadruple bond allows no spin pairing of the axial nitroxyl groups.

Acknowledgment. We thank the National Institutes of Health for partial support of the work at the University of Illinois through Grant HL 13652 to D.N.H.

Registry No. **1**, 91443-89-9; **2**, 91443-90-2; **3**, 91443-91-3; **4**, 91443-92-4; $\text{Rh}_2(\text{O}_2\text{CCF}_3)_4(\text{Tempo})_2$, 91443-93-5.

Supplementary Material Available: Listings of atomic positional parameters for **1** and **2**, and structure factor tables for **1** and **2** (33 pages). Ordering information is given on any current masthead page.

(24) The effects of strong axial donor atoms on the electronic structure are described in: (a) Cotton, F. A.; Bursten, B. E. *Inorg. Chem.* **1981**, *20*, 3042–3048. (b) Bursten, B. E.; Christoph, G. G.; Fox, L. S. *Inorg. Chem.*, in preparation.

(25) Shibaeva, R. N. *Zh. Strukt. Khim.* **1975**, *16*, 330–348; *J. Struct. Chem.* **1975**, *16*, 318–332 and references therein.

(26) (a) Cotton, F. A.; Extine, M.; Gage, L. D. *Inorg. Chem.* **1978**, *17*, 172–176. (b) Girolami, G. S.; Mainz, V. V.; Andersen, R. A. *Inorg. Chem.* **1980**, *19*, 805–810.

Chemical Derivatization of an Array of Three Gold Microelectrodes with Polypyrrole: Fabrication of a Molecule-Based Transistor

Henry S. White, Gregg P. Kittleson, and Mark S. Wrighton*

Department of Chemistry
Massachusetts Institute of Technology
Cambridge, Massachusetts 02139

Received April 30, 1984

We wish to report the fabrication of a chemically derivatized microelectrode array that can function as a transistor when immersed in an electrolyte solution. The key finding is that we have been able to show that a small signal (charge) needed to turn on the device can be amplified. The device to be described mimics the fundamental characteristics of a solid-state transistor,¹ since the resistance between two contacts can be varied by a signal to be amplified. Figure 1 illustrates the device fabricated and the external circuit elements needed to characterize it. The chemical transistor is the set of three (drain, gate, and source) Au microelectrodes covered with polypyrrole. Three features are essential: (1) the three independent Au microelectrodes are closely spaced, 1.4- μm apart, allowing an easily measurable current to pass between the source and drain when V_D is significant and V_G is above the threshold, V_T ; (2) the polypyrrole exhibits a sharp change in conductivity upon oxidation;² the potential at which this occurs is V_T ; (3) each of the microelectrodes can be individually contacted. The input signal to the gate to be amplified is that needed to oxidize the polypyrrole.³ Importantly, V_T and the magnitude of signal needed to achieve V_T can be manipulated by variation of the molecule-based material. Conceptually, the device described here stems from the molecule-based "diode" and "triode" fabricated by derivatizing a macroscopic electrode with a redox polymer and a porous metal outer contact.⁴ Additionally, the device represented in Figure 1 is a type of "chemiresistor"⁵ where an electrical signal can change the resistance of the chemical layer.

Experiments have been carried out using "chips" consisting of a microelectrode array of eight individual Au electrodes deposited on a 0.45 μm thick SiO_2 insulator grown on (100) Si. Each of the eight microelectrodes can be addressed independently and is generally 3 μm wide \times 140 μm long \times 0.12 μm thick separated from each other by 1.4 μm .⁶ Microelectrodes can be functionalized with controlled amounts of polypyrrole by oxidizing 50 mM pyrrole in $\text{CH}_3\text{CN}/0.1 \text{ M } [n\text{-Bu}_4\text{N}]\text{ClO}_4$ at +0.8 V vs. SCE, as described for macroscopic electrodes.² Microelectrodes derivatized in this manner can be characterized by cyclic voltammetry in $\text{CH}_3\text{CN}/0.1 \text{ M } [n\text{-Bu}_4\text{N}]\text{ClO}_4$, revealing the typical response expected for surface-bound polypyrrole.²

When the microelectrode array is derivatized with a sufficiently large coverage of polypyrrole, the individual microelectrodes can

(1) Sze, S. M. "Physics of Semiconductor Devices", 2nd ed.; Wiley: New York, 1981.

(2) (a) Kanazawa, K. K.; Diaz, A. F.; Geiss, R. H.; Gill, W. D.; Kwak, J. F.; Logan, J. A.; Rabolt, J.; Street, G. B. *J. Chem. Soc., Chem. Commun.* **1979**, 854–855. (b) Diaz, A. *Chem. Scr.* **1981**, *17*, 145–148. (c) Salmon, M.; Diaz, A. F.; Logan, J. A.; Krounki, M.; Bargon, J. *Mol. Cryst. Liq. Cryst.* **1982**, *83*, 265–276. (d) Diaz, A. F.; Martinez, A.; Kanazawa, K. K. *J. Electroanal. Chem.* **1981**, *130*, 181–187. (e) Bull, R. A.; Fan, F.-R. F.; Bard, A. J. *J. Electrochem. Soc.* **1982**, *129*, 1009–1015.

(3) The particular arrangement shown in Figure 1 has been used for clarity. Any one of the three electrodes could be used as a "gate" with the other two being "source" and "drain". Use of the gate electrode allows a quantitative determination of the amount of charge necessary to turn the polypyrrole from insulating (off) to conducting (on). Thus, the "gate" allows a quantitative assessment of the behavior of a two-electrode device where the input "signal" could be a redox reagent that equilibrates with the polypyrrole to turn it on. The arrangement in Figure 1 explicitly differs from solid-state transistors where both the gate and drain potentials are fixed relative to the source.¹ The crucial fact is that polypyrrole undergoes a dramatic change in conductivity upon transfer of a small amount of charge.

(4) Pickup, P. G.; Murray, R. W. *J. Electrochem. Soc.* **1984**, *131*, 833–839.

(5) For a recent overview of sensors that depend on microstructures, see: Wohljen, H. *Anal. Chem.* **1984**, *56*, 87A–103A.